A Global Climatology of $O_2 \cdot O_2$, $O_2 \cdot N_2$, and $(H_2O)_2$ Abundance and Absorption

C. S. Zender
National Center for Atmospheric Research
Boulder, Colorado

P. Chýlek
Atmospheric Science Program
Dalhousie University
Halifax, Canada

Introduction

Recent experimental and theoretical results show that the collision pairs, $O_2 \cdot O_2$ and $O_2 \cdot N_2$, absorb a small but significant fraction of the globally incident, solar radiation (Pfeilsticker et al. 1997, Solomon et al. 1998, Mlawer et al. 1998). The contribution of the water vapor dimer to shortwave (SW) absorption, however, remains speculative due to uncertainties in both its abundance and its absorption cross section (Chýlek and Geldart 1997, Clýlek et al. 1998, Tso et al. 1998). This study employs a specially modified version of the National Center for Atmospheric Research (NCAR) Community Climate Model, Version 3 (CCM3) general circulation model (GCM) to quantify the global abundances and SW radiative forcings of $O_2 \cdot X$ ($O_2 \cdot X \equiv O_2 \cdot O_2 + O_2 \cdot N_2$) and $(H_20)_2$, and the present uncertainties in these quantities.

Methods

Quantifying the global radiative forcing of a trace gas requires good characterization of both the global abundance and the spectral absorptance of the gas. In this study, all absorber abundances were computed every timestep (20 min.) in a 1-year integration of the NCAR CCM3 GCM. Monthly gridpoint biases in the CCM simulation of pressure, p, temperature, T, and water vapor, q_{H2O}, are generally much less than uncertainties in absorber cross section or abundance.

The abundance of $O_2 \cdot X$ is the product of the concentrations of O_2 and X, $[O_2]$ and [X], respectively. CCM gridpoint errors in monthly $[O_2]$ and $[N_2]$ are < 5%, and stem from biases in model p, T, and orography. The resulting uncertainty in $[O_2 \cdot O_2]$ and $[O_2 \cdot N_2]$ is < 10%.

The mass mixing ratio of $(H_2O)_2$ takes the form

$$q_{(H_2O)_2} = \mathrm{RH}\, q_{H_2O}\, a \exp(-b/T)\ \mathrm{kg\ kg^{-1}} \qquad (1)$$

where RH is relative humidity, and a = 144 and b = 3535 are parameters adjusted to fit experimental and *ab initio* model results (Chýlek et al. 1998). Other combinations of *ab initio* results and measurements predict $q_{(H2O)2}$ up to four times larger. Note that our $q_{(H2O)2}$ scales linearly with RH, even in clouds.

We employ $O_2 \cdot X$ binary absorption cross sections $\sigma_b(\lambda)$ from Solomon et al. (1998). The uncertainty in $\sigma_b(\lambda)$ is < 10% for $0.335 < \lambda < 1.137$ μm (Greenblatt et al. 1990). Uncertainty in 1.26 μm band absorption is ~ 30% (Solomon et al. 1998, Mlawer et al. 1998). We do not include absorption in the 1.58 μm band, which amounts to ~ 3% of $O_2 \cdot O_2$ absorption (Mlawer et al. 1998). The parameter, ε, defines the efficiency of N_2 relative to O_2 as a partner for inducing absorption in the O_2 1.26 μm band. These previous studies show $0.1 \le \varepsilon \le 0.3$, with the preponderance of studies suggesting $\varepsilon = 0.3$. We employ $\varepsilon = 0.2$.

Definitive laboratory measurements of $(H_2O)_2$ absorption cross sections $\sigma(\lambda)$ do not exist in the SW. We employ a 3-cm^{-1} resolution $\sigma(\lambda)$ from an *ab initio* model (Tso et al. 1998). The uncertainty in location of individual absorption bands is ~ 200 cm^{-1}. The large uncertainty in $\sigma(\lambda)$ contributes an uncertainty factor of 2-4 to total $(H_2O)_2$ broadband absorption.

In the SW, the CCM employs an 18-spectral bin δ-Eddington approximation (Briegleb 1992). We created $\overline{\sigma_i}$ for the CCM SW bins by spectrally averaging $\sigma_i(\lambda)$ from the source resolution to the CCM resolution. This procedure included weighting the high-resolution cross sections by the incident solar flux at the top of the atmosphere, and, in the case of $(H_2O)_2$, by the atmospheric

transmission simulated in a more detailed 1690 band Shortwave Narrowband (SWNB) model (Zender et al. 1997). The CCM $\overline{\sigma_i}$ were then tuned offline until CCM and SWNB absorption agreed for each absorber in atmospheric profiles ranging from the Arctic to the Tropics.

Results

The modified CCM was integrated for 12 months without any radiative feedback from the three new absorbers. $O_2 \cdot O_2$, $O_2 \cdot N_2$, and $(H_2O)_2$ abundances and instantaneous SW radiative forcings were diagnosed every timestep and output as monthly averages, from which the following annual averages were constructed. Except where noted, the qualitative features of $O_2 \cdot N_2$ abundance and absorption are the same as for $O_2 \cdot O_2$.

Annual Average Abundances and Forcings

Figure la shows the simulated annual average column abundance of $O_2 \cdot O_2$. The major meridional gradient in $O_2 \cdot O_2$ is caused by the poleward decrease in zonal average T. Arctic air is denser than tropical air, and because $[O_2 \cdot O_2]$ depends on the square of $[O_2]$, $[O_2 \cdot O_2]$ is ~ 20% greater in the Arctic than the Tropics at the same sea level pressure. The same would be true of the Antarctic, except the Antarctic plateau displaces the densest portion of the troposphere, significantly reducing $O_2 \cdot O_2$ column abundance. The Tibetan Plateau, Greenland, and the Andes also show significant orographic reduction in $[O_2 \cdot O_2]$. Note that orographic reduction of $[O_2 \cdot O_2]$ is time-invariant, in contrast to effects of seasonally varying T and p in the polar regions.

Figure lb shows the annual average SW radiative forcing of the atmosphere (increase in absorption) due to $O_2 \cdot X$. The annual forcing resembles the abundance, but some new features are evident. First, note the enhanced atmospheric absorption above bright, low surfaces (snow, desert, stratus clouds). Because the spectral optical depth of the $O_2 \cdot O_2$ bands is $\lesssim 0.02$, absorption in these bands is in the linear limit, where an increase in photon path length due to reflection causes a proportionate increase in atmospheric absorption. The zonal annual average atmospheric absorption due to $O_2 \cdot X$ is about 0.9 W m^{-2} and is nearly invariant with latitude (not shown).

Figure 2a shows the simulated annual average column abundance of $(H_2O)_2$. Since $[(H_2O)_2]$ depends on the square of $[H_2O]$, the poleward decrease in $[(H_2O)_2]$ is dictated by the square of the meridional gradient of the saturated vapor

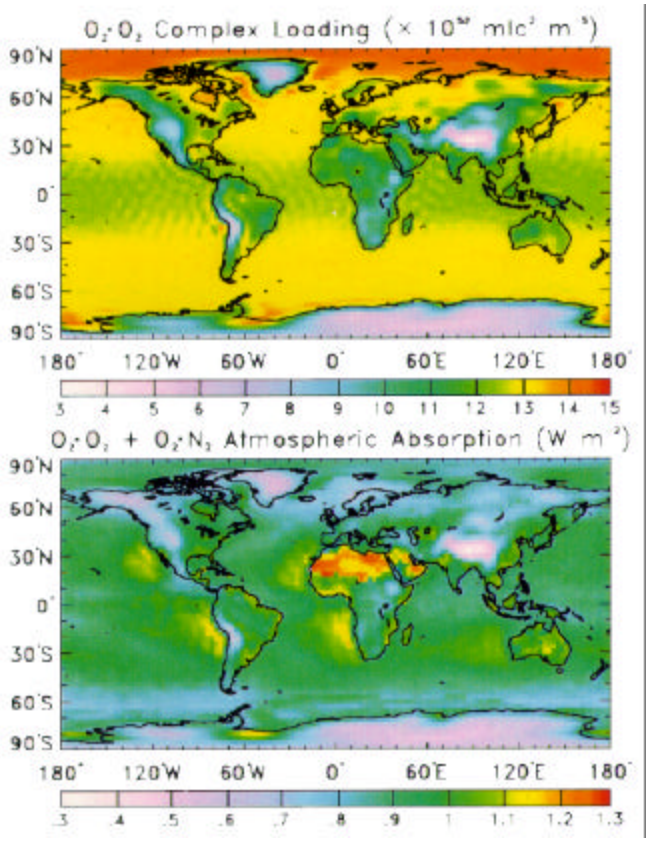

Figure 1. (a) Annual average column abundance (mlc^2 m^{-5}) of $O_2 \cdot O_2$. (b) Annual average instantaneous change in atmospheric absorption (W m^{-2}) due to $O_2 \cdot O_2$. (For a color version of this figure, please see *http://www.arm.gov/docs/documents/technical/conf_9803/zender-98.pdf*.)

pressure, q_s, in the lower troposphere. q_s varies exponentially with surface temperature, so the poleward decline in $[(H_2O)_2]$ is quite strong. Zonal annual average $(H_2O)_2$ absorption (not shown) in the Tropics (averaged 20 °S to 20 °N) is 1.83 W m^{-2}, roughly 3.5 times greater than in the Northern mid-latitudes (averaged 30 °N to 50 °N). The intertropical convergence zone (ITCZ) and continental centers of deep convection appear as the regions of strongest forcing.

The global average statistics for Figures 1 and 2 are summarized in Tables 1 and 2. Note that the global annual average clear-sky atmospheric forcing by $(H_2O)_2$ is predicted to exceed the cloudy-sky forcing by nearly 20%. This is because all clouds except low stratus shield more $(H_2O)_2$ beneath them from solar radiation than there is $(H_2O)_2$ above them. Of course, if an unknown mechanism were producing more $(H_2O)_2$ than we assume within clouds [Eq. (1)], this would not necessarily be the case.

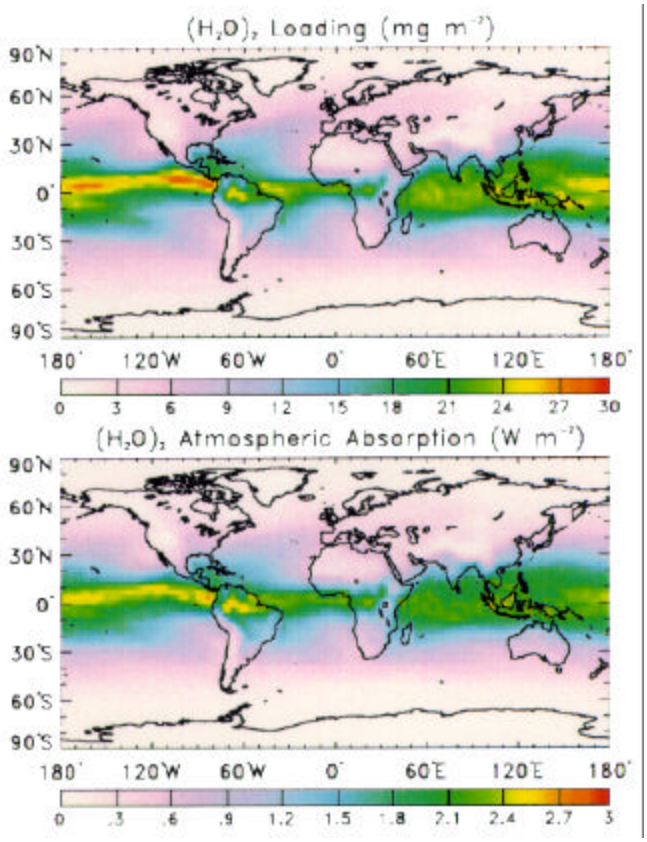

Figure 2. As in Figure 1 but for (a) $(H_2O)_2$ abundance (mg m^{-2}). (b) Atmospheric absorption due to $(H_2O)_2$. (For a color version of this figure, please see *http://www.arm.gov/docs/documents/technical/conf_9803/zender-98.pdf*.)

Table 1. Global annual average abundances.

Absorber	Units	Abundance	Uncertainty
$O_2 \cdot O_2$	$mlc^2\ cm^{-5}$	1.2×10^{43}	± 10%
$O_2 \cdot N_2$	$mlc^2\ cm^{-5}$	4.6×10^{43}	± 10%
$(H_2O)_2$	$mlc\ cm^{-2}$	1.66×10^{16}	1-4 ×
$(H_2O)_2$	mg m^{-2}	9.9	1-4 ×

Table 2. Global annual average forcings (W m^{-2}).

Forcings (W m^{-2})	$O_2 \cdot O_2$	$O_2 \cdot N_2$	$(H_2O)_2$
Atmospheric absorption	0.78	0.15	0.96
(same, but for clear sky)	(0.78)	(0.17)	(1.14)
Surface absorption	-0.42	-0.08	-0.69
Sfc. + atm. absorption	0.36	0.07	0.28
Surface insolation	-0.50	-0.10	-0.76

Seasonal Patterns of Abundances and Forcings

Due to the seasonal cycle of solar insolation and the natural variability of organized tropical convection, annual average forcings alone do not suffice to characterize the geographic and vertical distribution of the forcings as they impact the climate system. We present Northern Summer (June-July-August, or JJA) seasonal average forcings in Figure 3.

Figure 3a shows the simulated JJA average radiative forcing of $O_2 \cdot X$. Most remarkable is the large polar region where atmospheric $O_2 \cdot X$ absorption exceeds 1.5 W m^{-2}. $O_2 \cdot X$ forcing peaks in the polar summer, when peak solar insolation coincides with the largest $O_2 \cdot X$ abundances (Figure 1a). Antarctic Summer forcings (not shown) are nearly symmetric about the equator in Figure 3.

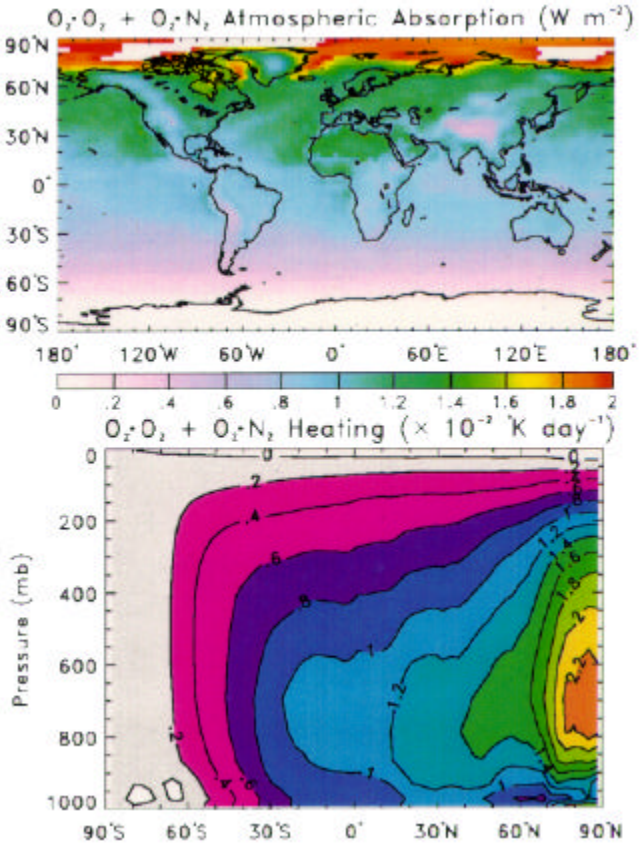

Figure 3. Seasonal average instantaneous radiative forcing in Northern Summer (JJA average) due to $O_2 \cdot O_2 + O_2 \cdot N_2$. (a) Atmospheric absorption (W m^{-2}). (b) Heating rate ($\times 10^{-02}$ °K day^{-1}). (For a color version of this figure, please see *http://www.arm.gov/docs/documents/technical/conf_9803/zender-98.pdf*.)

Equinoctial forcings (not shown) extend farther into the winter hemisphere than solsticial forcings, and are weaker.

Figure 3b shows the vertical distribution of the simulated JJA average, zonal average, and SW radiative heating due to $O_2 \cdot X$. Seasonal $O_2 \cdot O_2$ heating in excess of 0.02 °K/day^{-1} extends throughout the Arctic troposphere. This is 2% to 5% of local SW heating due to all other absorbers. The heating decreases vertically due to decreasing $[O_2 \cdot X]$, and decreases southward due to decreasing daylight hours. Heating in the Antarctic summer troposphere is similar, but slightly stronger, probably due to higher surface albedo. Most GCMs have strong cold biases at the summertime polar tropopause. It is likely that allowing $O_2 \cdot X$ radiative feedbacks will ameliorate, though not eliminate these biases.

Figure 4a shows the simulated JJA average radiative forcing of $(H_2O)_2$. The southwest monsoon over the Indian subcontinent dominates the zonal signature of $(H_2O)_2$ absorption, and the ITCZ also stands out. $(H_2O)_2$ absorption should be most evident at the Atmospheric Radiation Measurement (ARM) Cloud and Radiation Testbed (CART) site during this season. Figure 4b shows the concomitant $(H_2O)_2$ heating distribution. Heating due to $(H_2O)_2$ is strongest in the lower troposphere, reaching nearly 0.1 °K day^{-1} in the Asian Monsoon and ITCZ regions. $(H_2O)_2$ heating reaches its greatest vertical and northward extents during JJA. Heating during other seasons (not shown) is otherwise very similar.

Conclusions

The global distributions of $[O_2 \cdot O_2]$ and $[O_2 \cdot N_2]$ depend most on zonal average T, p, and orography. $O_2 \cdot X$ absorbs approximately 0.93 W m^{-2} of incident solar radiation with a strong seasonal and meridional dependence. This absorption is comparable to the anthropogenic forcing of important greenhouse gases. Because of this, and the relatively small uncertainties in $O_2 \cdot X$ abundance and cross sections, $O_2 \cdot X$ should be implemented in GCMs. $O_2 \cdot X$ has the most potential to improve the simulated climate in summertime polar regions.

The distribution of $(H_2O)_2$ centers on regions of organized deep convection such at the ITCZ and monsoon regions. $(H_2O)_2$ heating is centered in the lower tropical troposphere. The absolute abundance of $(H_2O)_2$ is still poorly known, as is its absorption cross section. Using our set of assumptions, $(H_2O)_2$ forcing is comparable to $O_2 \cdot X$. The large uncertainties involved make it premature to implement $(H_2O)_2$ in GCMs. Further laboratory and *ab initio* studies of $(H_2O)_2$ properties are warranted.

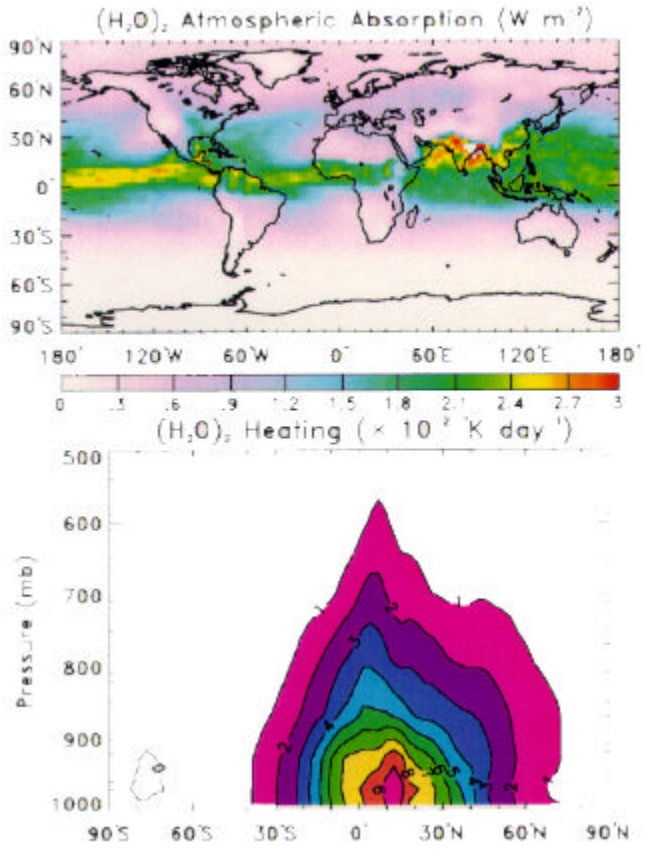

Figure 4. As in Figure 3 but for $(H_2O)_2$. (For a color version of this figure, please see *http://www.arm.gov/docs/documents/technical/conf_9803/zender-98.pdf*.)

References

Briegleb, B. P., 1992: Delta-Eddington approximation for solar radiation in the NCAR community climate model. *J. Geophys. Res.*, **97**(D7), 7603-7612.

Chýlek, P., and D. J. W. Geldart, 1997: Water vapor dimers and atmospheric absorption of electromagnetic radiation. *Geophys. Res. Lett.*, **24**, 2015-2018.

Greenblatt, G. D., J. J. Orlando, J. B. Burkholder, and A. R. Ravishankara, 1990: Absorption measurements of oxygen between 330 and 1140 nm. *J. Geophys. Res.*, **95**(D11), 18,577-18,582.

Mlawer, E. J., S. A. Clough., P. D. Brown, T. M. Stephen, J. C. Landry, A. Goldman, and F. J. Murcray, 1998: Observed atmospheric collision-induced absorption in near-infrared oxygen bands. *J. Geophys. Res.*, **103**(D4), 3859-3863.

Pfeilsticker, K., F. Erle, and U. Platt, 1997: Absorption of solar radiation by atmospheric O_4. *J. Atmos. Sci.*, **54**(7), 933-939.

Solomon. S., R. W. Portmann, R. W. Sanders, and J. S. Daniel, 1998: Absorption of solar radiation by water vapor, oxygen, and related collision pairs in the Earth's atmosphere. *J. Geophys. Res.*, **103**(D4), 3847-3858.

Tso, H. C. W., J. W. Geldart, and P. Chýlek, 1998: Anharmonicity and cross-section for absorption of radiation by water dimer. *J. Chem. Phys*., **108**, 5319.

Zender, C. S., B. Bush, S. K. Pope, A. Bucholtz, W. D. Collins, J. T. Kiehl, F. P. J. Valero, and J. Vitko, Jr., 1997: Atmospheric absorption during the Atmospheric Radiation Measurement (ARM) Enhanced Shortwave Experiment (ARESE). *J. Geophys. Res.*, **102**(D25), 29,901-29,915.

Other Publications in Progress

Chýlek, P., Q. Fu, H. C. W. Tso, and D. J. W. Geldart, 1998: Contribution of water vapor dimers to clear sky absorption of solar radiation. In preparation.